CORROSION SCIENCE AND TECHNOLOGY, Vol.5, No.2(2006), pp.77~83

# Mechanical Properties and Corrosion Resistance of Plasma Electrolytic Oxidation Coatings on AZ31 Magnesium Alloy

**Jae Seon Park, Hwa Chul Jung, and †Kwang Seon Shin**

*School of Materials Science and Engineering, Seoul National University*
*San 56-1, Sillim-dong, Gwanak-gu, Seoul 151-744, Korea*

The plasma electrolytic oxidation (PEO) process is a relatively new surface treatment technique that produces a chemically stable and environment-friendly electrolytic coating that can be applied to all types of magnesium alloys. In this study, the characteristics of oxide film were examined after coating the extruded AZ31 alloy through the PEO process. Hard ceramic coatings were obtained on the AZ31 alloy by changing the coating time from 10min to 60min. The morphologies of the surface and the cross-section of the PEO coatings were examined by scanning electron microscopy and optical microscopy, and the thickness of the coating was measured. The X-ray diffraction pattern of the coating shows that the coated layer consists mainly of the MgO and $Mg_2SiO_4$ phases after the oxidation reaction. The hardness of the coated AZ31 alloy increased with increasing coating time. In addition, the corrosion rates of the coated and uncoated AZ31 alloys were examined by salt spray tests according to ASTM B 117 and the results show that the corrosion resistance of the coated AZ31 alloy was superior to that of the un-coated AZ31 alloy.

***Keywords*** *: magnesium alloy; plasma electrolytic oxidation, hardness; salt spray test; corrosion resistance*

## 1. Introduction

The interest in the structural applications of lightweight materials has increased significantly due to their importance in the environmental pollution and energy saving problems. The consumption of magnesium alloys has particularly increased in the automobile and electronic industries during the past decade due to their low density, high specific strength and recyclability. However, the application field of magnesium alloys has been rather limited because of their poor corrosion resistance. In recent years, the modification of alloy composition and/or heat treatment has been attempted to improve the corrosion resistance of Mg alloys.[1)-4)] However, there is a growing need for better surface treatment techniques for magnesium alloys in order to significantly improve the corrosion resistance which is required in a wide range of applications. A number of surface treatment techniques such as electroplating, conversion coating, gas-phase deposition and anodizing have been developed to prevent the corrosion of Mg alloys.[5)]

The plasma electrolytic oxidation (PEO) process is a relatively new surface treatment technique which offers a number of distinct advantages compared to other traditional processes. It provides a surface film which has improved hardness, corrosion and wear resistance and higher fatigue strength than those obtained by traditional processes. In the PEO process, a plasma environment is generated and a ceramic coating can be synthesized on the metal surface through plasma chemical interactions.[6),7)] The PEO process has been used to produce hard ceramic coatings on light metals such as Al, Ti, Mg, and their alloys.[8)-12)] It has been reported that the dense and hard PEO coatings formed on magnesium alloys significantly improved the wear and corrosion resistance.[9),13)] In the present study, the effects of coating time on the characteristics of the coated layer were examined after coating the extruded AZ31 Mg alloy by the PEO process. The morphologies of the surface and the cross-sections of the PEO layers, as well as the thickness of the coating, were examined as a function of coating time. The hardness and corrosion resistance of the AZ31 alloy after different coating times were also examined and compared with those of the un-coated AZ31 alloy.

†Corresponding author: ksshin@snu.ac.kr

## 2. Experimental procedures

### 2.1 Production of the AZ31 alloy sheet and the PEO process

The AZ31 alloy was melted in a low carbon steel crucible while the melt surface was protected with a gas mixture of $CO_2$ + 0.5% $SF_6$. The melt was mechanically stirred for 1 hour, and the crucible was directly quenched into cold water. The ingot was homogenized at 400℃, water-cooled, and subsequently machined to a billet with a 77 mm diameter and 140 mm length. After preheating, the billet was extruded by a horizontal indirect extrusion machine to a sheet with 30 mm width and 3 mm thickness.

The extruded AZ31 alloy sheets were cut to the size of 30 mm x 20 mm x 3 mm for the subsequent PEO experiments. All specimens were mechanically polished with SiC papers and 0.3㎛ alumina powders, cleaned in ethanol and dried in warm air before they were subjected to the PEO coating process. In the present study, a 9 kW plasma electrolytic oxidation equipment, which consisted of a pulse AC power supplier, an electrolyte bath, a cooling and stirring system for electrolyte, appropriate electrodes and a sample holder, was used for the coating experiments. The PEO process involves the creation of plasma discharge around a specimen immersed in an electrolyte. A modulated AC voltage is applied to the specimen, creating intense plasma due to micro-arc generation at the specimen surface. This results in oxidation of the specimen surface with co-deposition from the electrolyte.[14] A low concentration alkaline solution was used as an electrolyte in the present PEO process. Important process parameters in the PEO coating process are the composition of the electrolyte, current density, electrolyte temperature, current wave, and coating time. In the present study, all experiments were conducted under constant PEO coating conditions; a current density of 0.2 A/cm$^2$, a current ratio of 1 : 0.1 and an electrolyte temperature of 20℃. The coating time was varied from 10 min to 60 min in order to examine the changes in the characteristics of the PEO layers with coating time. The PEO coating process on the extruded AZ31 alloy sheet is shown in Fig. 1.

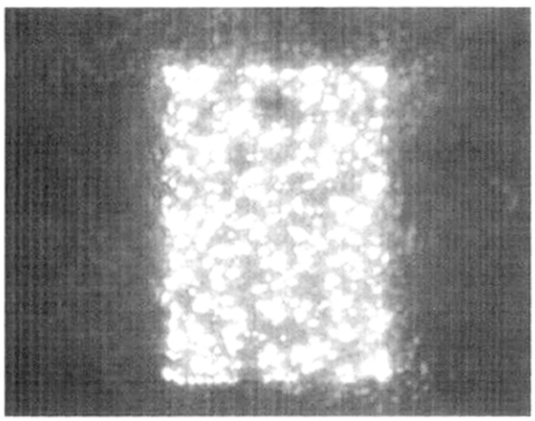

**Fig. 1.** The PEO coating process on the extruded AZ31 alloy sheet.

### 2.2 Characterization of the PEO coatings

The changes in the morphologies of the surface and the cross-section of the PEO coatings were examined by a JSM-6360 scanning electron microscope (SEM) and an OPTIPHOT-100 optical microscope (OM), and the thickness of the coated layer was measured. A M18XHF-SRA X-ray diffractometer (50kW, 100mA, CuK$\alpha$ radiation) was used to analyze the phases in the PEO layer. The hardness of the coated layer was measured on the polished cross-section by a Fischerscope H100C micro-hardness testing system with an applied load of 200 mN and a loading/unloading time of 20 sec. The corrosion rates of the coated AZ31 alloys were examined by salt spray tests according to the ASTM B 117. The salt spray test was performed in a 5 wt.% NaCl aqueous solution (6.8 pH) at 35℃ for 240 hours. The corrosion rate was determined from the change in weight in mpy (mils per year):

$$corrosionRate(mpy) = \frac{534W}{DAT} \quad (1)$$

where W is weight loss in milligrams, D is density in grams per cubic centimeter, A is area in square inches and T is time in hours.

## 3. Results and discussion

### 3.1 Observation of the surface/cross-section morphology and thickness measurement of coatings

In this study, the change in surface morphology was examined with coating time. The scanning electron micrographs in Fig. 2(a)~(f) show the changes in surface morphology of the PEO coatings on the AZ31 alloy substrates as the coating time increased from 10 min to 60 min.

The surface morphology of the PEO coating was reported to show non-uniform spherical lamellar pieces like volcano tops formed on the surface with a large number of pores.[15),16)] In the present study, the PEO coatings on the AZ31 alloy show similar shapes as those observed in the PEO coatings of other alloys. The change in the surface morphology of oxide coatings was investigated to determine the effect of coating time. It was found that the

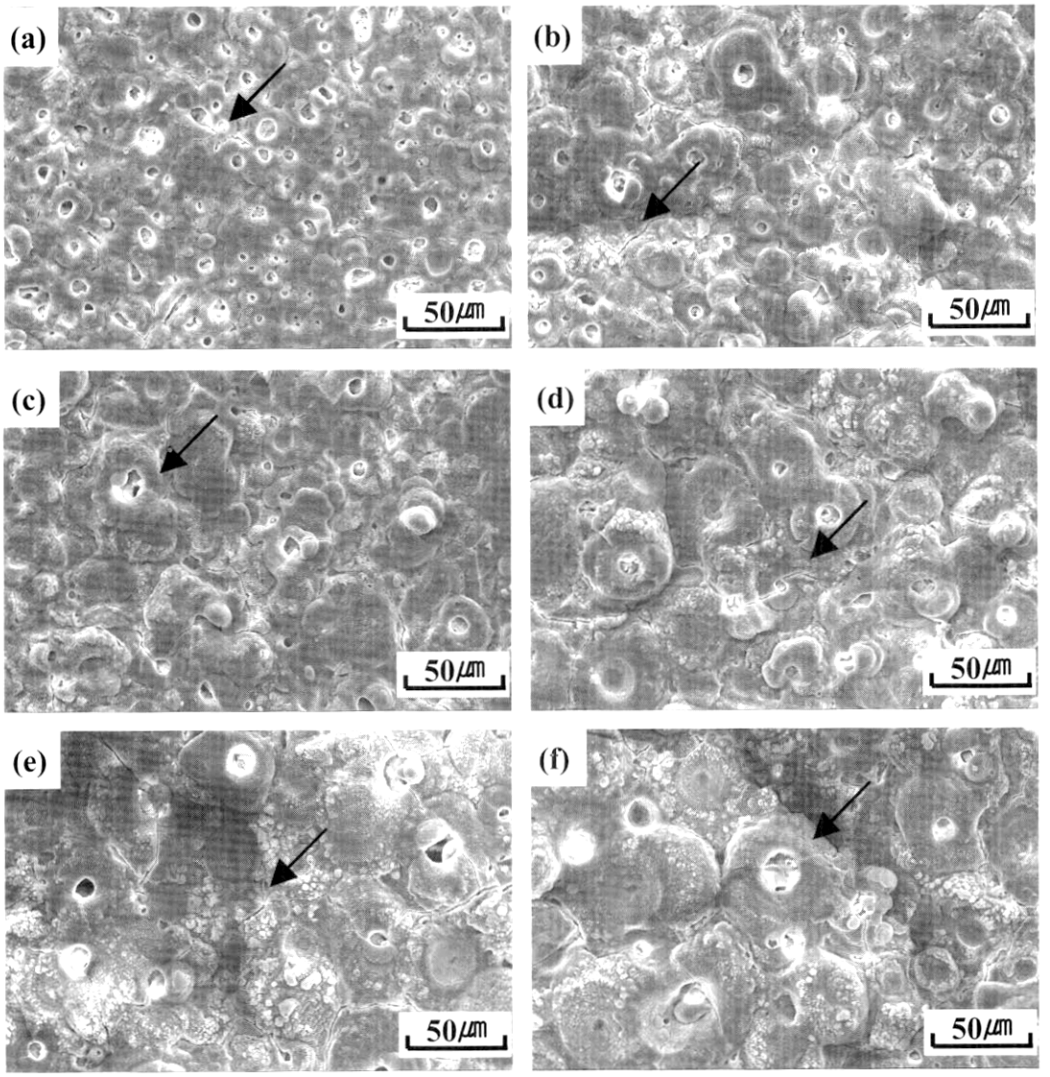


**Fig. 2.** Surface morphologies of the PEO coatings on the AZ31 alloy with different coating times; (a) 10min, (b) 20min, (c) 30min, (d) 40min, (e) 50min and (f) 60min.

coatings on the extruded AZ31 alloy sheet have much larger pore sizes and smaller pore number with increasing coating time. The average pore diameter of the PEO coatings increased from 8.8 $\mu$m to 18.8 $\mu$m as the coating time increased from 10 min to 60 min. In addition, the oxide particle size in the coated layer increased in proportion to coating time. It is considered that this phenomenon is attributed to the continuous increase of voltage with coating time, which promotes the conversion of the fine arc discharges to larger arc discharges and decreases the number of arc discharges.

Wei *et al.* reported that microcracks appear on the coated surface, which can be initiated due to the thermal stress caused by the rapid solidification of the melted products in the discharge channel.[15] Similar microcracks were also observed at the surface of the PEO coatings on the AZ31 alloy, as shown by the arrows in Fig. 2.

Fig. 3 shows the optical micrographs of the polished cross-sections of the PEO coatings with change in coating time. In the figure, the AZ31 alloy substrate is shown as the bright part and the PEO layer is the middle part between the substrate and the mounting resin. Typical cross-section morphology of the PEO coatings showed that the coated layers were not fully compact.

The average thickness of the PEO coating was determined from the optical micrographs obtained from the cross-section of the coated layers. Fig. 4 shows the variation in the thickness of the PEO layer with change in coating time. The thickness of the PEO layer increases proportionally with coating time. The formation rate of

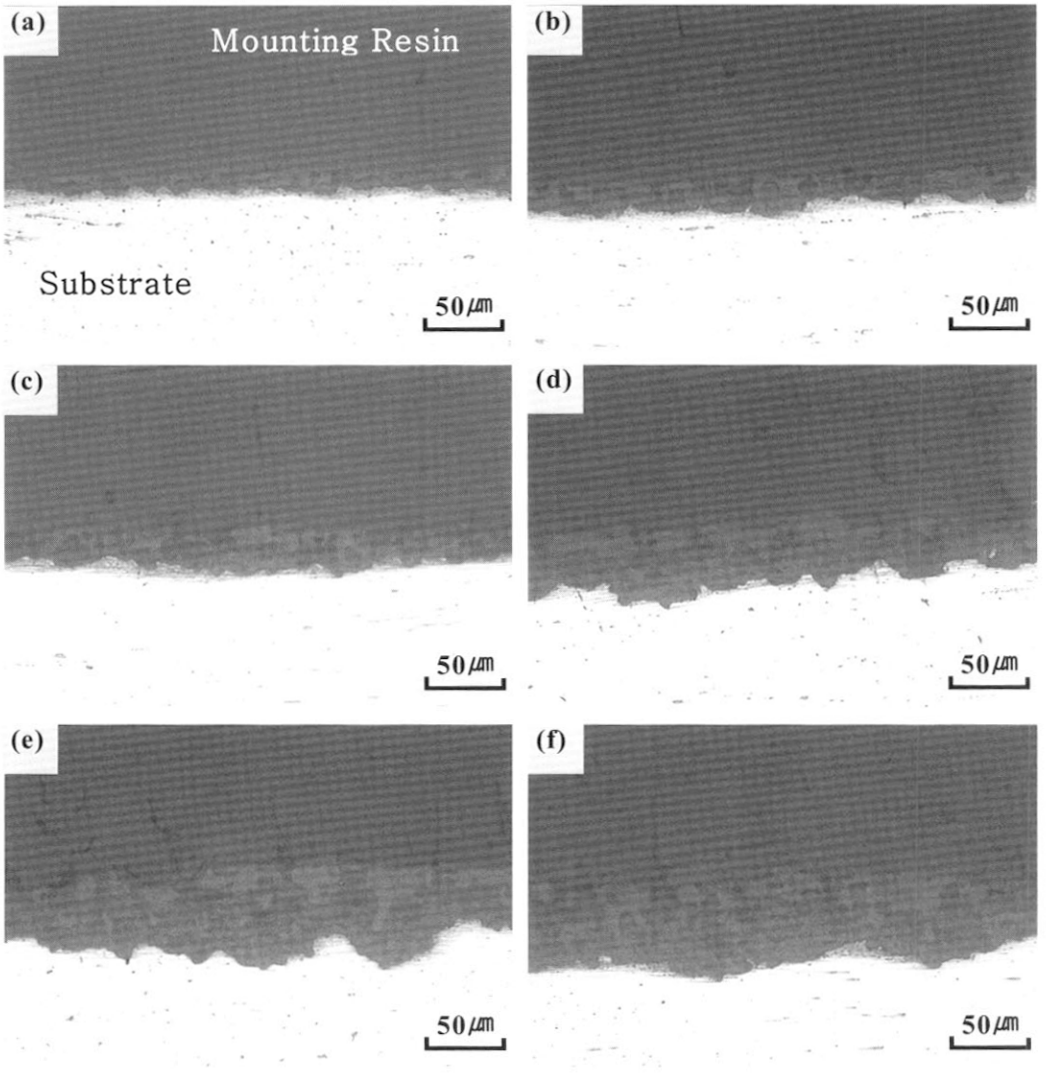


**Fig. 3.** Cross-section morphologies of the PEO coatings on the AZ31 alloy with different coating times; (a) 10min, (b) 20min, (c) 30min, (d) 40min, (e) 50min and (f) 60min.

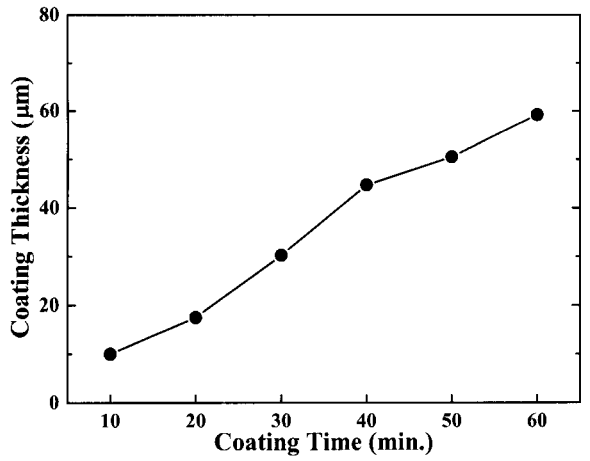


**Fig. 4.** Change in the coating thickness with coating time.

the layer was found to be approximately 1 μm/min under the coating conditions used in this study.

### 3.2 Phase analysis of the PEO coatings

Fig. 5 shows an X-ray diffraction pattern of the PEO layer on the AZ31 alloy. Apelfeld *et al.* reported that the coatings produced by the PEO process consist of the MgO and $Mg_2SiO_4$ phases due to the formation of the complex mixture of the oxides of the elements present both in magnesium alloy (Mg, Al, Mn, Zn) and in the electrolyte (Na, Si).[17] In the present study, the X-ray diffraction pattern of the PEO layer confirmed the formation of the magnesium oxide (MgO) and high hardness forsterite ($Mg_2SiO_4$) phases, and the natural magnesium mineral. The most important factor determing the phases in the

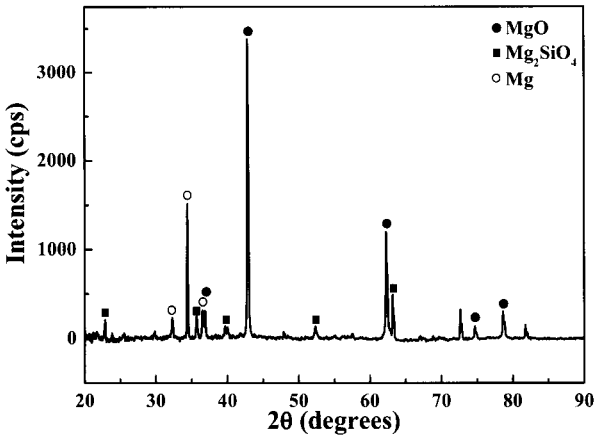


**Fig. 5.** X-ray diffraction pattern of the PEO coatings on the AZ31 alloy.

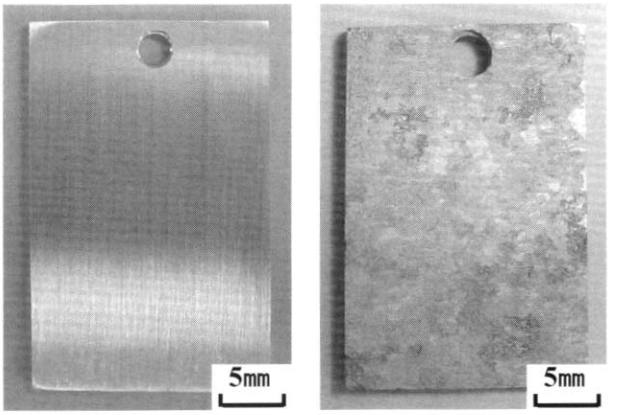


**Fig. 7.** Photographs of the un-coated AZ31 Mg alloy; (a) before 240hr salt spray test and (b) after 240hr salt spray test.

coated layer is a variety of elements in the magnesium alloy and in the electrolyte, which decides the type of phase in the PEO layer.

### 3.3 Hardness measurement of the PEO coatings

Fig. 4 shows the change in the micro-hardness of the PEO layer with change in coating time. Shrestha *et al.* reported that hardness ranging from 345 $H_V$ to 446 $H_V$ was obtained from the PEO layer consisting of the $MgAl_2O_4$, $SiO_2$ and $SiP_2$ phases on the AZ91 alloy substrate.[15] Liang *et al.* reported a hardness of about 600 $H_V$ from the PEO layer consisting of the MgO, $Mg_2SiO_4$, $MgAl_2O_4$, $MgF_2$ and $KMgF_2$ phases on the AM60 alloy substrate.[18] As shown in Fig. 6, the micro-hardness of the PEO layer on the AZ31 alloy increased from 350 $H_V$ to 660 $H_V$ with increasing the coating time from 10 min to 60 min. These hardness values are five to nine times higher than that of the extruded AZ31 alloy substrate (about 71$H_V$). A similar tendency was also observed in the PEO coating of other Mg alloys.

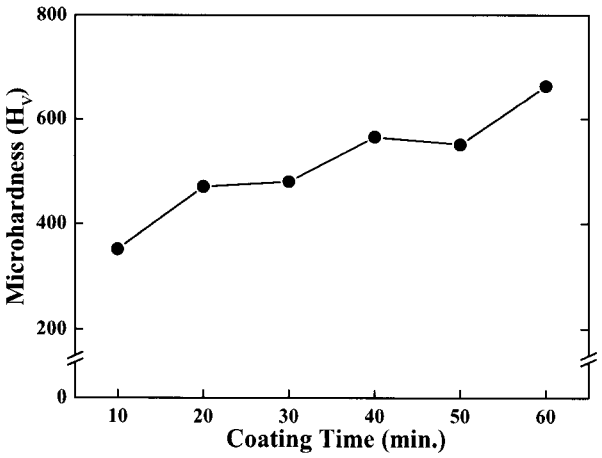


**Fig. 6.** Micro-hardness of the PEO coatings with increasing coating time.

### 3.4 Salt spray test

A salt spray test was used in order to examine the effects of the PEO layer on corrosion resistance. Fig. 7 and Fig. 8 show the surface morphology of the un-coated AZ31 alloy and the coated AZ31 alloy before and after a 240 hour salt spray test. As seen in Fig. 7 (b), the un-coated AZ31 alloy specimen after a 240 hour salt spray test showed visible corrosion products. However, the coated AZ31 alloy did not show any visible corrosion products on the exposed surface regardless of coating time as shown in Fig. 8. The corrosion rates were determined from the change in weight in mpy (mils per year). The results of these measurements are shown in Fig. 9. The corrosion rates of the coated AZ31 alloy were significantly lower than that of the un-coated AZ31 alloy, and the corrosion rate decreased with increasing coating time. It appeared that the corrosion rate of the coated AZ31 alloy is three to forty-eight times lower than that of the un-coated AZ31 alloy. The coated AZ31 alloy shows a remarkable improvement in corrosion resistance compared to the un-coated AZ31 alloy.

## 4. Summary

The plasma electrolytic oxidation (PEO) coating of the AZ31 alloy sheet was carried out, and the following conclusions can be made from the present study.

1) The PEO coating on the AZ31 alloy substrate is a porous layer. The size of pores increases with increasing coating time, while the number of pores decreases.

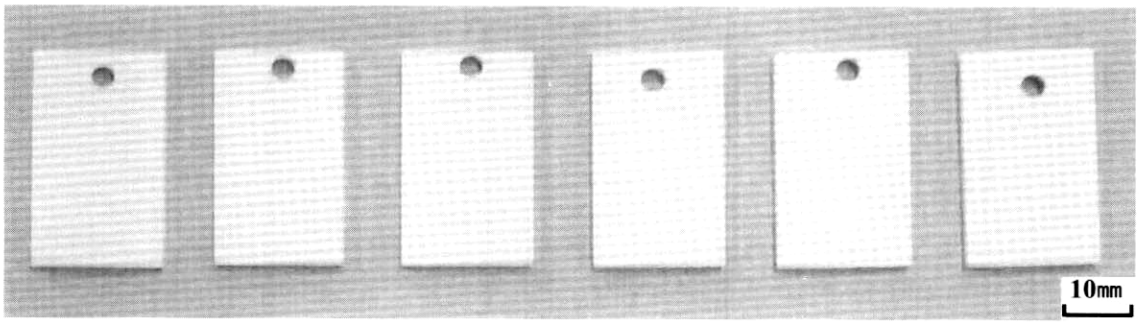


(a)

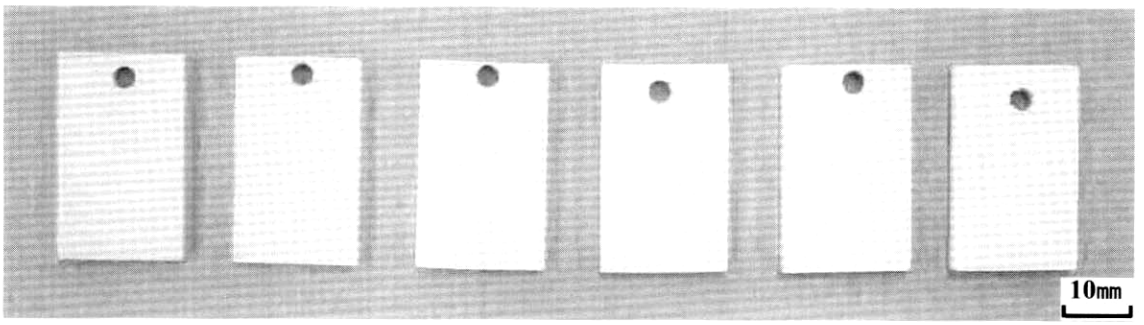


(b)

**Fig. 8.** Photographs of the PEO coated AZ31 alloy; (a) before 240hr salt spray test and (b) after 240hr salt spray test. (from left after 10min, 20min, 30min, 40min, 50min and 60min coating)

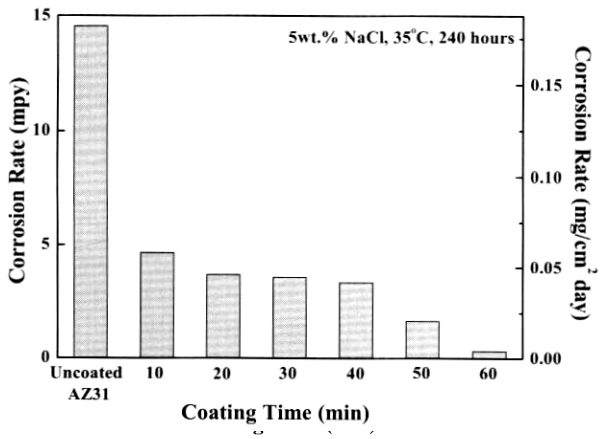


**Fig. 9.** Corrosion rates of AZ31 alloys at different PEO coating times.

2) The thickness of the PEO layer increases proportionally with increasing coating time. The formation rate of the layer was approximately 1$\mu$ m/min under the PEO conditions used in this study.

3) The X-ray diffraction pattern of the coated layer on the AZ31 alloy substrate confirmed the formation of the magnesium oxide (MgO) and high hardness forsterite ($Mg_2SiO_4$) phases.

4) The hardness of the PEO coatings was five to nine times higher than that of the extruded AZ31 alloy substrate (about $71H_V$).

5) From the results of salt spray tests, it was found that the corrosion rate of the coated AZ31 alloy was three to forty-eight times lower than that of the un-coated AZ31 alloy. The coated AZ31 alloy showed remarkable improvement in corrosion resistance compared to the un-coated AZ31 alloy.

## Acknowledgements

This work was financially supported by the Korean Ministry of Commerce, Industry and Energy through the Dual Technology Program.

## References

1. C. D. Lee, C. S. Kang, and K. S. Shin, *Met. Mater.*, **6**, 351 (2000).
2. C. D. Lee, C. S. Kang, and K. S. Shin, *Met. Mater.*, **6**, 441 (2000).
3. C. D. Lee, C. S. Kang, and K. S. Shin, *Met. Mater.-Int.*, **7**, 385 (2001).
4. Y. J. Ko, C. D. Yim, J. D. Lim, and K. S. Shin, Mater.

Sci. Forum, **419-422**, 851 (2003).
5. J. E. Gray and B. Luan. J. Alloys Comp., **336**, 88 (2002).
6. A. L. Yerokhin, X. Nie, A. Leyland, A. Mattews and S.J. Dowey, *Surf. Coat. Technol.*, **122**, 73 (1999).
7. A. L. Yerokhin, V. V. Lyubimov, and R. V. Ashitkov, *Ceram. Int.*, **122**, 1 (1999).
8. W. Krysmann, P. Kurze, K. H. Dittrich, and H. G. Schneider, *Cryst. Res. Technol.*, **19**(7), 973 (1984).
9. X. Nie, E. I. Meletis, J. C. Jiang, A. Leyland, A. L. Yerokhin, and A. Matthews, *Surf. Coat. Technol.*, **149**, 245 (2002).
10. A. L. Yerokhin, X. Nie, A. Leyland, and A. Mattews, *Surf. Coat. Technol.*, **130**, 195 (2000).
11. A. L. Yerokhin, X. Nie, A. Leyland, and A. Mattews, *Appl. Surf. Sci.*, **200**, 172 (2002).
12. A. Kuhn, *Met. Finishing*, **101**(9), 44 (2003).
13. A. J. Zozulin and D. E. Bartak, *Met. Finishing*, **92**(3), 39 (1994).
14. S. Shrestha, A. Sturgeon, P. Shashkov, and A. Shatrov, Magnesium Technology 2002, 283 (2002).
15. T. Wei, F. Yan, and J. Tian, *J. Alloys Comp.*, **389**, 169 (2005).
16. A. L. Yerokhin, A. Shatrov, V. Samsonov, P. Shashkov. A. Leyland, and A. Matthews, *Surf. Coat. Technol.*, **182**, 78 (2004).
17. A. V. Apelfeld, O. V. Bespalova, A. M. Borisov, O. N. Dunkin, N. G. Goryaga, V. S. Kulikauskas, E. A. Romanovsky, S. V. Semenov and I. V. Souminov, Nuclear Instruments and Methods in Physics Research, **B 161-163**, 553 (2000).
18. J. Liang, B. Guo, J. Tian, H. Liu, J. Zhou, and T. Xu, *Appl. Surf. Sci.*, **252**, 345 (2005).